AMERICAN SOCIETY FOR MICROBIOLOGY | Infection and Immunity®

CELLULAR MICROBIOLOGY:
PATHOGEN-HOST CELL MOLECULAR INTERACTIONS

Redistribution of the Novel *Clostridioides difficile* Spore Adherence Receptor E-Cadherin by TcdA and TcdB Increases Spore Binding to Adherens Junctions

Pablo Castro-Córdova,[a]* Macarena Otto-Medina,[b] Nicolás Montes-Bravo,[a] Christian Brito-Silva,[a] D. Borden Lacy,[c] Daniel Paredes-Sabja[a,d]

[a]ANID-Millennium Science Initiative Program-Millennium Nucleus in the Biology of the Intestinal Microbiota, Santiago, Chile
[b]Departamento de Ciencias Biológicas, Facultad de Ciencias de la Vida, Universidad Andrés Bello, Santiago, Chile
[c]Department of Pathology, Microbiology, and Immunology, Vanderbilt University School of Medicine, Nashville, Tennessee, USA
[d]Department of Biology, Texas A&M University, College Station, Texas, USA

Pablo Castro-Córdova, Macarena Otto-Medina, and Nicolás Montes-Bravo contributed equally to this work. Authors order was determined by increasing seniority.

ABSTRACT *Clostridioides difficile* causes antibiotic-associated diseases in humans, ranging from mild diarrhea to severe pseudomembranous colitis and death. A major clinical challenge is the prevention of disease recurrence, which affects nearly ~20 to 30% of the patients with a primary *C. difficile* infection (CDI). During CDI, *C. difficile* forms metabolically dormant spores that are essential for recurrence of CDI (R-CDI). In prior studies, we have shown that *C. difficile* spores interact with intestinal epithelial cells (IECs), which contribute to R-CDI. However, this interaction remains poorly understood. Here, we provide evidence that *C. difficile* spores interact with E-cadherin, contributing to spore adherence and internalization into IECs. *C. difficile* toxins TcdA and TcdB lead to adherens junctions opening and increase spore adherence to IECs. Confocal micrographs demonstrate that *C. difficile* spores associate with accessible E-cadherin; spore-E-cadherin association increases upon TcdA and TcdB intoxication. The presence of anti-E-cadherin antibodies decreased spore adherence and entry into IECs. By enzyme-linked immunosorbent assay (ELISA), immunofluorescence, and immunogold labeling, we observed that E-cadherin binds to *C. difficile* spores, specifically to the hairlike projections of the spore, reducing spore adherence to IECs. Overall, these results expand our knowledge of how *C. difficile* spores bind to IECs by providing evidence that E-cadherin acts as a spore adherence receptor to IECs and by revealing how toxin-mediated damage affects spore interactions with IECs.

KEYWORDS *C. difficile* spores, E-cadherin, adherens junctions, exosporium

Clostridioides difficile is a Gram-positive, anaerobic, spore-forming bacterium and the main causative agent of antibiotic-associated diarrhea, causing death in ~5% of cases (1, 2). A major clinical challenge in C. difficile infections (CDI), is recurrence of CDI (R-CDI), affecting ~30% of CDI patients (2, 3). CDI is primarily driven by the *C. difficile* toxins TcdA and TcdB, with contributions from the binary transferase toxin in some cases (4–6). Both TcdA and TcdB target their intracellular glucosyltransferase activity toward RhoA, Rac1, and Cdc42 (7, 8). This inhibitory modification of the Rho GTPase family leads to actin depolymerization and disruption of tight and adherens junctions (9–13), causing disruption of epithelial paracellular barrier function (14). Clinical studies showed that administration of anti-TcdB antibody (bezlotoxumab) in combination with antibiotics reduces R-CDI rates (15), through mechanisms that remain unclear.

During infection, *C. difficile* produces spores (16). Strains unable to form spores do not cause R-CDI in animal models (17), indicating that the spores are critical for R-CDI.

Editor Nancy E. Freitag, University of Illinois at Chicago

Address correspondence to Daniel Paredes-Sabja, dparedes-sabja@bio.tamu.edu.

*Present address: Pablo Castro-Córdova, IMPACT, Center of Interventional Medicine for Precision and Advanced Cellular Therapy, Santiago, Chile.

The authors declare no conflict of interest.

Received 20 October 2022
Accepted 20 October 2022
Published 30 November 2022

EDTA disruption of cell-cell junctions in Caco-2 cells leads to increased adherence of *C. difficile* spores at the cell-cell junction, suggesting a tropism for cell-cell junctions (18). Indeed, *C. difficile* spores bind to fibronectin and vitronectin, located in the basolateral membrane (19). These molecules contribute to *C. difficile* spore internalization into IECs in an integrin-dependent manner, and *in vivo* spore entry contributes to R-CDI (20).

The intestinal barrier is an impermeable layer that separates the apical and basolateral cell sides (21) and is formed by junctions between adjacent IECs. The cell-cell junctions between IECs are constituted of E-cadherin-containing adherens junctions and tight junctions formed by claudins, occludens, and zonula occludens. These junctions provide the gut barrier with impermeability properties and restrict the translocation of pathogens and commensal bacteria. However, some pathogens can alter or disrupt the cell junctions to translocate through the host (22).

Several enteric pathogens such as *Streptococcus pneumoniae*, *Fusobacterium nucleatum*, *Campylobacter jejuni*, and *Listeria monocytogenes* take advantage of disrupted intestinal adherens junctions to internalize in host cells (23–27). How *C. difficile* spores interact with adherens junctions remains poorly described. Here, we show that accessible E-cadherin is reduced in differentiated Caco-2 cells. Also, TcdA and TcdB intoxication increases spore adherence, which is correlated with an increase in E-cadherin accessibility in IECs. Next, we observed that *C. difficile* spores interact with E-cadherin in healthy IECs and the binding is increased in TcdA- and TcdB-intoxicated cells. Also, the blocking of the cellular E-cadherin with monoclonal antibodies reduces spore adherence and entry to IECs. Finally, we observed that E-cadherin binds to the hairlike extensions of the exosporium.

RESULTS

Characterization of accessible E-cadherin in monolayers of Caco-2 cells. Caco-2 cells have been employed to assess *C. difficile* interaction with IECs (18–20, 28–32). Early work demonstrated that *C. difficile* spores had a tropism toward the cell-cell junction of EDTA-treated Caco-2 cells (18). Therefore, to understand the dynamic of adherens junction closure during Caco-2 cell differentiation, we assessed the accessibility of E-cadherin in undifferentiated and differentiated monolayers of Caco-2 cells. First, Caco-2 cell differentiation was assessed for the appearance of microvilli by transmission electron microscopy (TEM) and sucrase-isomaltose as a differentiation marker in monolayers cultured for 2 or 8 days postconfluence (19). Next, differentiated and undifferentiated Caco-2 cells were immunostained for accessible E-cadherin (using an antibody that detects an extracellular domain of Ecadherin, followed by fluorescent-labeled secondary antibody) (Fig. 1A and B). Results demonstrate that in undifferentiated Caco-2 cells, ~84% of the cells were immunolabeled for accessible E-cadherin (Fig. 1C), whereas in differentiated Caco-2 cells, only ~7% of the cells were stained for accessible E-cadherin (Fig. 1C). As a control, cells were permeabilized and stained for total E-cadherin, and we observed that ~100% of both undifferentiated and differentiated Caco-2 cells were immunolabeled for E-cadherin (Fig. 1D to E). These results demonstrate that after 8 days of differentiation, most of the cells lack accessible E-cadherin (Fig. 1F).

Intoxication with *C. difficile* TcdA and TcdB increases accessible E-cadherin. Studies have shown that *C. difficile* toxins TcdA and TcdB cause tight and adherens junction dissociation (9–11). Interestingly, TcdA, but not TcdB, causes a displacement of E-cadherin from the cell-cell junctions to be located around the cells in Caco-2 cells (11), while in the colonic epithelium, TcdB causes adherens junctions disruption (10). Since most of the *C. difficile* strains causing disease produce TcdA and TcdB (33), we asked whether TcdA and TcdB affect the accessibility of E-cadherin in differentiated Caco-2 cells. Thus, TcdA- and TcdB-intoxicated differentiated Caco-2 cells for 3, 6, and 8 h were immunostained for accessible E-cadherin (nonpermeabilized). For total E-cadherin staining, cells were permeabilized and immunostained with the same primary antibody and a fluorescent-labeled secondary antibody with another Alexa Fluor dye (see Materials and Methods). Next, we acquired confocal micrographs, and the

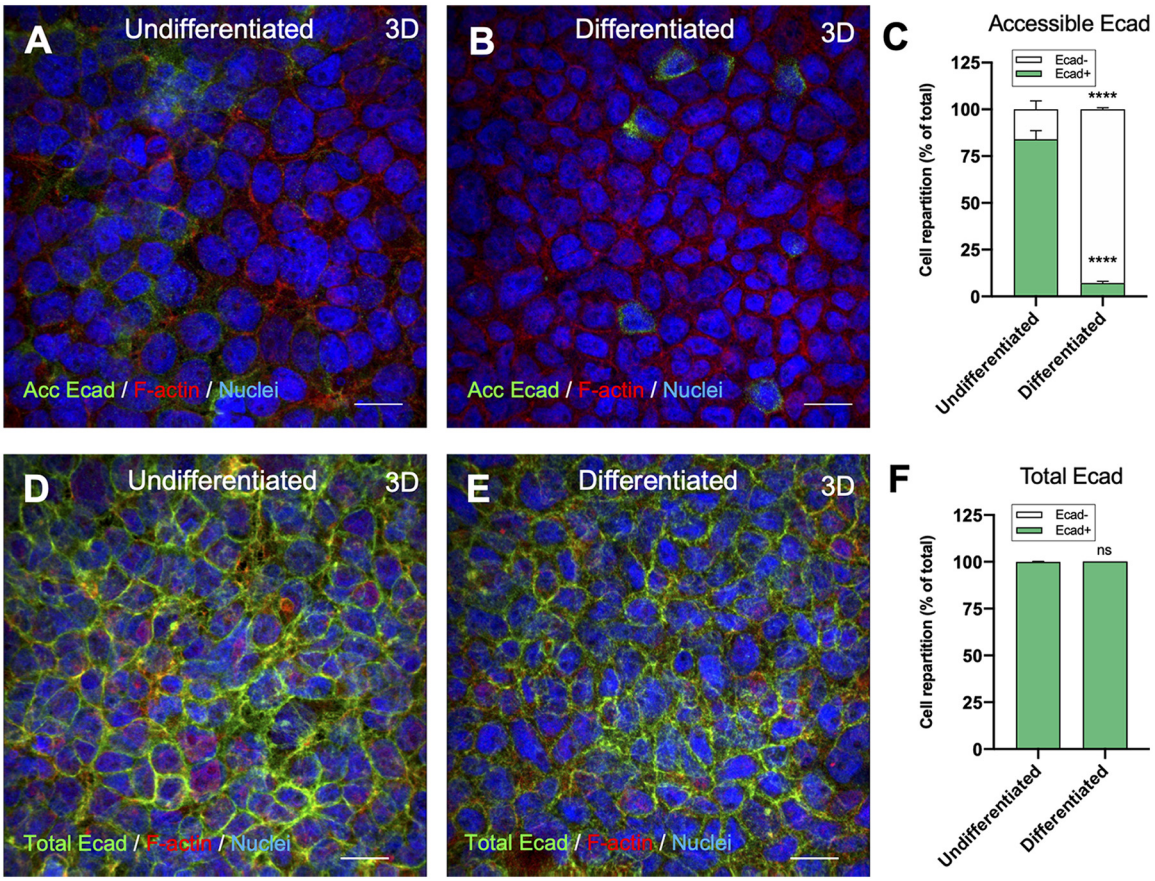

FIG 1 Distribution of accessible and total E-cadherin in undifferentiated and differentiated Caco-2 cells. Three-dimensional projections of a representative confocal micrograph of healthy undifferentiated (A) and differentiated (B) Caco-2 cells immunostained for accessible E-cadherin. Accessible E-cadherin (shown as acc Ecad) is in green, F-actin in red, and nuclei in blue. (C) Repartition of cells that were positive (Ecad+) or negative (Ecad−) stained for accessible E-cadherin. (D and E) Three-dimensional projection of a representative confocal micrograph of healthy undifferentiated (D) and differentiated (E) Caco-2 cells immunostained for total E-cadherin. (F) Repartition of cells that were positive (Ecad+) or negative (Ecad−) stained for total E-cadherin. Fluorophores colors were digitally reassigned for a better representation. Micrographs are representative of 6 fields of 2 independent experiments. Scale bar, 20 μm. Error bars indicate mean ± SEM. Statistical analysis was performed by two-tailed unpaired Student's *t* test. ns, $P > 0.05$; ****, $P \leq 0.0001$.

fluorescence intensity was quantified for every slice of the z-stack for accessible and total E-cadherin. The sum of the fluorescence intensity of accessible E-cadherin was significantly higher (175% relative to unintoxicated monolayers) after 8 h intoxication (Fig. 2A and B). To evaluate if this increase of fluorescence intensity occurs in the apical or basal half of the monolayer, we split the number of slices of the z-stack into 2 halves (apical and basal) with the same number of slices. We summed the fluorescence intensity for accessible E-cadherin in the apical (Fig. 2C) or basal (Fig. 2D) halves of the monolayer. We observed a significant increase in accessible E-cadherin fluorescence intensity in both the apical and basal halves, 177% and 176%, respectively, after 8 h intoxication (Fig. 2C and D). Using the same strategy, we quantified the total E-cadherin fluorescence intensity in the complete *z*-stack, and we observed a significant decrease of 19% after 6 h and an increase of 12.2% after 8 h intoxication compared to unintoxicated cells (Fig. 2E). Then, we observed that these variations were in the apical and not in the basal half of the monolayer. We observed a decrease of 35% after 6 h and an increase of 44% after 8 h intoxication compared to unintoxicated cells (Fig. 2F and G). To confirm the degree of TcdA and TcdB intoxication, we evaluated the glucosyltransferase activity by measuring the levels of glucosylated Rac1 in TcdA- and TcdB-intoxicated differentiated and undifferentiated monolayers using strategies previously described (34). After 3 h of intoxication, no modification of Rac1 was observed.

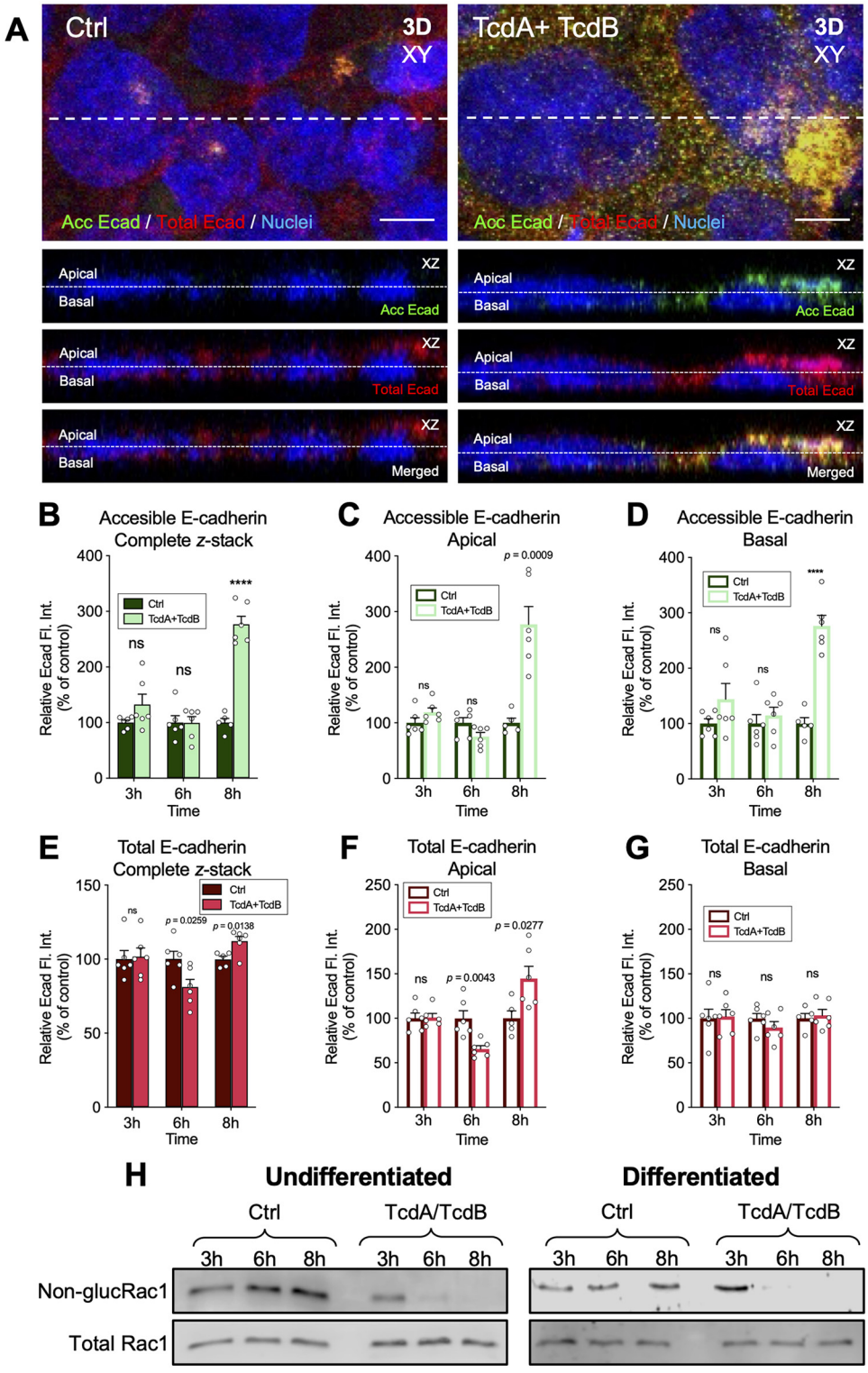

FIG 2 The accessibility of E-cadherin increases in TcdA- and TcdB-intoxicated IECs. Differentiated TcdA- and TcdB-intoxicated Caco-2 cells for 3, 6, or 8 h in DMEM without serum. As a control, cells were incubated with DMEM without serum. Nonpermeabilized cells were stained for accessible E-cadherin (shown as acc Ecad; green) and permeabilized, and total E-cadherin was stained (shown as total Ecad; red) and nuclei (blue). (A) Representative confocal microscopy images in 3D (*xy*) projection of control cells (left) and TcdA- and TcdB-intoxicated cells for 8 h (right); below the orthogonal view (*xz*; accessible E-cadherin, total E-cadherin, and merged) of the dotted line of the *xy*. Representative confocal images for 3 h and 8 h not shown. (B to D) Relative fluorescence intensity measured as the sum of each z-step of accessible E-cadherin (B) and its abundance in the apical side (C) or in the basal side (D) of

(Continued on next page)

However, after 6 and 8 h of intoxication, the unglucosylated Rac1 signal disappeared, indicating a complete glucosylation of Rac1 (Fig. 2H). These results indicate that the cells were fully intoxicated by 6 h, and accessible E-cadherin is increased in differentiated Caco-2 cells after 8 h intoxication.

***C. difficile* toxins TcdA and TcdB increase adherence to IECs.** Several studies have shown that vegetative *C. difficile* adherence to IECs is enhanced following TcdA or CDT intoxication (11, 35, 36). To expand the understanding of how intoxication of IECs impacts spore adherence, differentiated and undifferentiated Caco-2 cells were TcdA and TcdB intoxicated for 8 h or incubated for 8 h with heat-inactivated TcdA and TcdB as a control. Then undifferentiated and differentiated cells were infected for 3- and 1 h, respectively, with *C. difficile* spores in the absence of serum. Cells were fixed and immunostained without permeabilization. In TcdA- and TcdB-intoxicated Caco-2 cells, we observed more adhered spores than in unintoxicated cells or than in cells incubated with heat-inactivated TcdA/TcdB (Fig. 3A). After quantitative analysis, we observed in undifferentiated Caco-2 cells that spore adherence in 8-h TcdA- and TcdB-intoxicated cells was ~105% higher than in unintoxicated monolayers, and no differences in spore adherence were observed in cells 8 h incubated with heat-inactivated TcdA and TcdB (Fig. 3B). Similarly, in differentiated cells, we observed an increase of ~321% in 8-h TcdA- and TcdB-intoxicated cells over that in unintoxicated monolayers, and no differences were observed in cells 8 h incubated with heat-inactivated TcdA and TcdB (Fig. 3C). Collectively, these data indicate that TcdA and TcdB intoxication of undifferentiated and differentiated Caco-2 cells increases *C. difficile* spore adherence.

Intoxication of IECs increases *C. difficile* spore association with E-cadherin. Since we observed that TcdA- and TcdB-intoxicated differentiated Caco-2 cells lead to an increase of accessible E-cadherin and adherence of *C. difficile* spores, we tested whether this could be attributed to *C. difficile* spores associating with accessible E-cadherin. For this, unintoxicated or 8-h TcdA- and TcdB-intoxicated differentiated Caco-2 cells were infected with *C. difficile* spores for 1 h. Then, accessible E-cadherin and spores were immunostained and visualized by confocal microscopy (Fig. 4A and D). Plot profile analysis of unintoxicated Caco-2 cells (Fig. 4A) reveals that ~21% of adhered *C. difficile* spores were associated with accessible E-cadherin (Fig. 4B, C, and G). Notably, upon TcdA and TcdB intoxication (Fig. 4D), ~72% of adhered spores were associated with accessible E-cadherin (Fig. 4E to G). These results indicate that adhered *C. difficile* spores can associate with accessible E-cadherin in IECs, and this association is enhanced upon TcdA and TcdB intoxication.

Antibody blocking of accessible E-cadherin reduces adherence and internalization of *C. difficile* spores to IECs. Next, we assessed whether E-cadherin is involved in *C. difficile* spore adherence and internalization. We have shown that *C. difficile* spore internalization occurs in the presence of serum (20). Therefore, undifferentiated, differentiated, and polarized Caco-2 cells were incubated with anti-E-cadherin antibody for 2 h and subsequently infected for 3- (undifferentiated cells) and 1-h (differentiated cells) with fetal bovine serum (FBS)-incubated *C. difficile* spores. To identify intracellular spores, we used the intracellular spore exclusion immunostaining assay (20), where only extracellular spores are immunostained in nonpermeabilized cells, and total spores are visualized by phase-contrast microscopy. Using this strategy in undifferentiated Caco-2 cells, we observed that *C. difficile* spore adherence to IECs was significantly decreased upon increasing concentrations of anti-E-cadherin antibody; spore adherence decreased by 38,

FIG 2 Legend (Continued)
the cell. (E to G) Relative fluorescence intensity of total E-cadherin (E) and its abundance in the apical side (F) and the basal side (G) of the cell. Controls were set at 100%. Error bars indicate the mean ± SEM from at least 9 fields ($n = 3$). (H) Immunoblotting of anti-nonglucosylated Rac1 and total Rac1 of cell lysates of undifferentiated and differentiated Caco-2 cells intoxicated with TcdA and TcdB for 3, 6, or 8 h. For undifferentiated and differentiated Caco-2 cells, nonglucosylated Rac1 was evaluated with corresponding antibodies, then the membrane was stripped, and subsequently tested for total Rac1. Western blotting is representative of 3 independent experiments. Statistical analysis was performed by two-tailed unpaired Student's *t* test. ns, $P > 0.05$; ****, $P < 0.0001$. Bars, 5 μm. Fl.Int., fluorescence intensity.

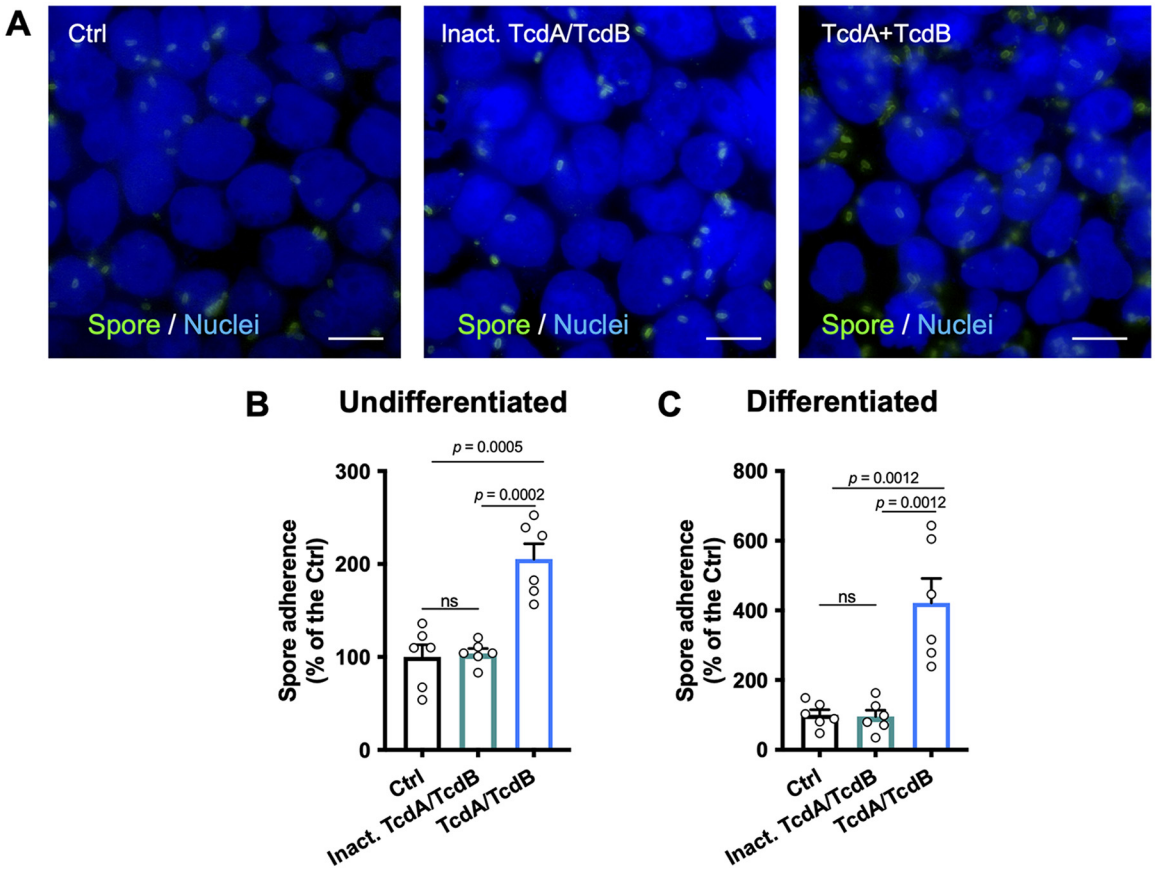

FIG 3 TcdA and TcdB increase *C. difficile* spore interaction with IECs. Caco-2 cells were differentiated and TcdA and TcdB intoxicated for 8 h or incubated with DMEM without serum as control and then were washed with PBS and infected for 3 h (Undifferentiated cells) or 1 h (differentiated cells) at an MOI of 10 with *C. difficile* spores. Unbound spores were rinsed off. Nonpermeabilized cells were stained for adhered spores. (A) Representative epifluorescence microscopy images of TcdA- and TcdB-intoxicated cells, cells incubated with heat inactivated TcdA/TcdB (or DMEM as control) for 8 h, which were then washed and infected with *C. difficile* spores. (B and C) *C. difficile* spore adherence relative in undifferentiated (B) and differentiated (C) cells. In bars, each dot represents one independent well from 2 independent experiments. Per well, a total of 5 fields were analyzed. Error bars indicate the mean ± SEM. Statistical analysis was performed by unpaired *t* test. ns, $P > 0.05$. Bars, 10 μm.

53, and 73% compared to the control when cells were incubated with 1, 10, and 100 μg mL^{-1} of anti-E-cadherin antibody, respectively (Fig. 5A). Upon quantifying internalization in undifferentiated Caco-2 cells, we observed a significant decrease of 38, 43, and 69% compared to the control in cells incubated with 1, 10, and 100 μg mL^{-1} of anti-E-cadherin, respectively (Fig. 5B). Similarly, in differentiated Caco-2 cells, a significant decrease in spore adherence in 18, 32, 60, and 70% compared to the control was observed in cells incubated with 0.1, 1, 10, and 100 μg mL^{-1} of anti-E-cadherin, respectively (Fig. 5C). For internalization, we observed a significant decrease in 15, 35, 42, and 54% compared to the control in cells incubated with 0.1, 1, 10, and 100 μg mL^{-1} of anti-E-cadherin, respectively (Fig. 5D). Finally, in polarized Caco-2 cells, we observed a decrease in 32, 56, 63, and 79% in spore adherence compared to the control in presence with 0.1, 1, 10, and 100 μg mL^{-1} of anti-E-cadherin, respectively (Fig. 5E). These data indicate that the antibody-mediated blockage of accessible E-cadherin reduces *C. difficile* spore adherence and internalization to IECs.

Purified recombinant human E-cadherin competitively inhibits spore adherence in undifferentiated, differentiated, and TcdA- and TcdB-intoxicated IECs cells. Subsequently, to provide further evidence that E-cadherin acts as a spore adherence receptor, we evaluated infected un-intoxicated undifferentiated Caco-2 monolayers with *C. difficile* spores preincubated with 1, 2.5, 5, 10, and 25 μg mL^{-1} of E-cadherin, and we observed a decrease in spore adherence of 12%, 26%, 38%, 47%, and 64%, respectively, compared to spores not incubated with E-cadherin (Fig. 6A). In differentiated Caco-2 cells,

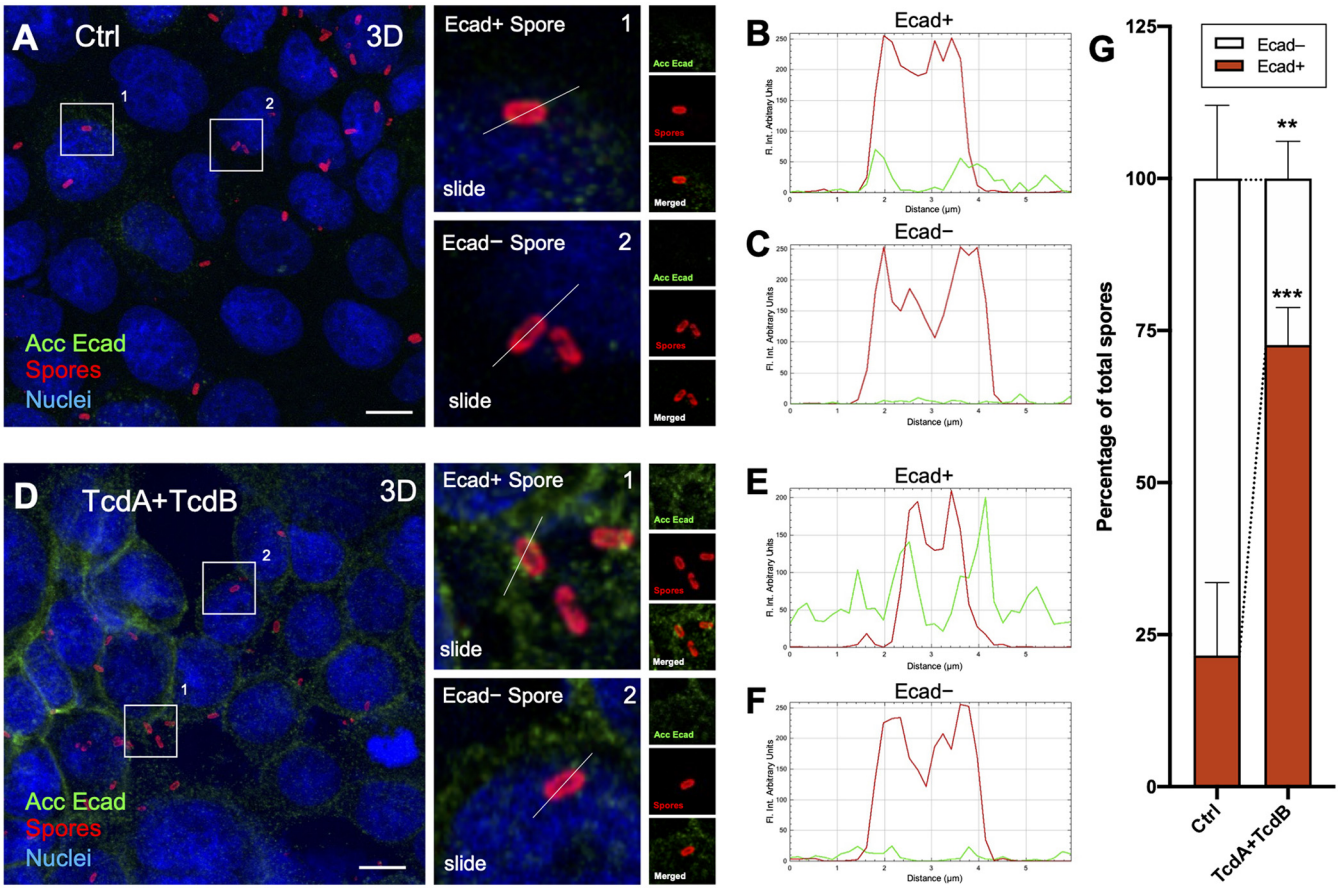

FIG 4 E-cadherin of IECs interacts with increasing *C. difficile* spores in TcdA- and TcdB-intoxicated cells. Differentiated Caco-2 cells were intoxicated with TcdA and TcdB for 8 h at 37°C in DMEM without serum. As a control, cells were incubated with DMEM without serum. Then, cells were infected with *C. difficile* spores for 1 h at 37°C. Nonpermeabilized cells were stained for accessible E-cadherin (shown as acc Ecad; green), spores (red), and nuclei (blue). (A) Representative 3D projection confocal micrograph of healthy cells infected with *C. difficile* spores (Ctrl). (A, Right) Magnifications of representative *C. difficile* spores associated or not with E-cadherin. (B and C) Plot profiles of fluorescence intensity of *C. difficile* spores (red line) and accessible E-cadherin (shown as Ecad, green line) performed in the white line of panel A. (D) Representative 3D projection confocal micrograph of TcdA- and TcdB-intoxicated cells infected with *C. difficile* spores. (D, Right) Magnifications of representative *C. difficile* spores associated or not with E-cadherin. (E and F) Plot profiles of fluorescence intensity of *C. difficile* spores (red) and accessible E-cadherin (shown as Ecad, in green) performed in the white line of panel D. Repartition of spores that were positive (Ecad+) or negative (Ecad−) associated with fluorescence signal for accessible E-cadherin was shown as the average associated/nonassociated spores with E-cadherin for each field; a total of ~500 spores were analyzed. Fluorophores were digitally reassigned for a better representation. Micrographs are representative of 6 independent fields of 3 different experiments. Error bars indicate mean ± SEM. Statistical analysis was performed by two-tailed unpaired Student's *t* test. $P \leq 0.01$; ***, $P \leq 0.001$. Bars, 10 μm.

we observed a decrease in spore adherence of 27%, 30%, 30%, 27%, and 53% for spores incubated with 1, 2.5, 5, 10, and 25 μg mL^{-1} of E-cadherin, respectively (Fig. 6B). Finally, we also assessed whether the increased spore adherence that we previously observed in TcdA- and TcdB-intoxicated Caco-2 cells was E-cadherin specific. As expected, significant *C. difficile* spore adherence to TcdA- and TcdB-intoxicated Caco-2 cells was observed in the absence of E-cadherin; however, upon intoxication of TcdA- and TcdB-intoxicated differentiated and undifferentiated Caco-2 cells with spores previously incubated with 25 μg mL^{-1} of E-cadherin for 1 h at 37 °C, and we observed a significant decrease of 41% in undifferentiated (Fig. 6C) and 55% in differentiated Caco-2 cells (Fig. 6D) compared to TcdA- and TcdB-intoxicated cells. Overall, these results show that E-cadherin interacts with *C. difficile* spores in a dose-dependent manner and that competition experiments with purified E-cadherin reduce the *C. difficile* spore adherence in healthy and intoxicated cells.

E-cadherin binds in a concentration-dependent manner to *C. difficile* spores. To provide evidence that *C. difficile* spores interact with E-cadherin, we used enzyme-linked immunosorbent assay (ELISA) with *C. difficile* spore-coated wells incubated with increasing concentrations of E-cadherin or BSA as a control. E-cadherin binding activity was evident in *C. difficile* spore-coated wells (Fig. 7A). The specificity of this interaction

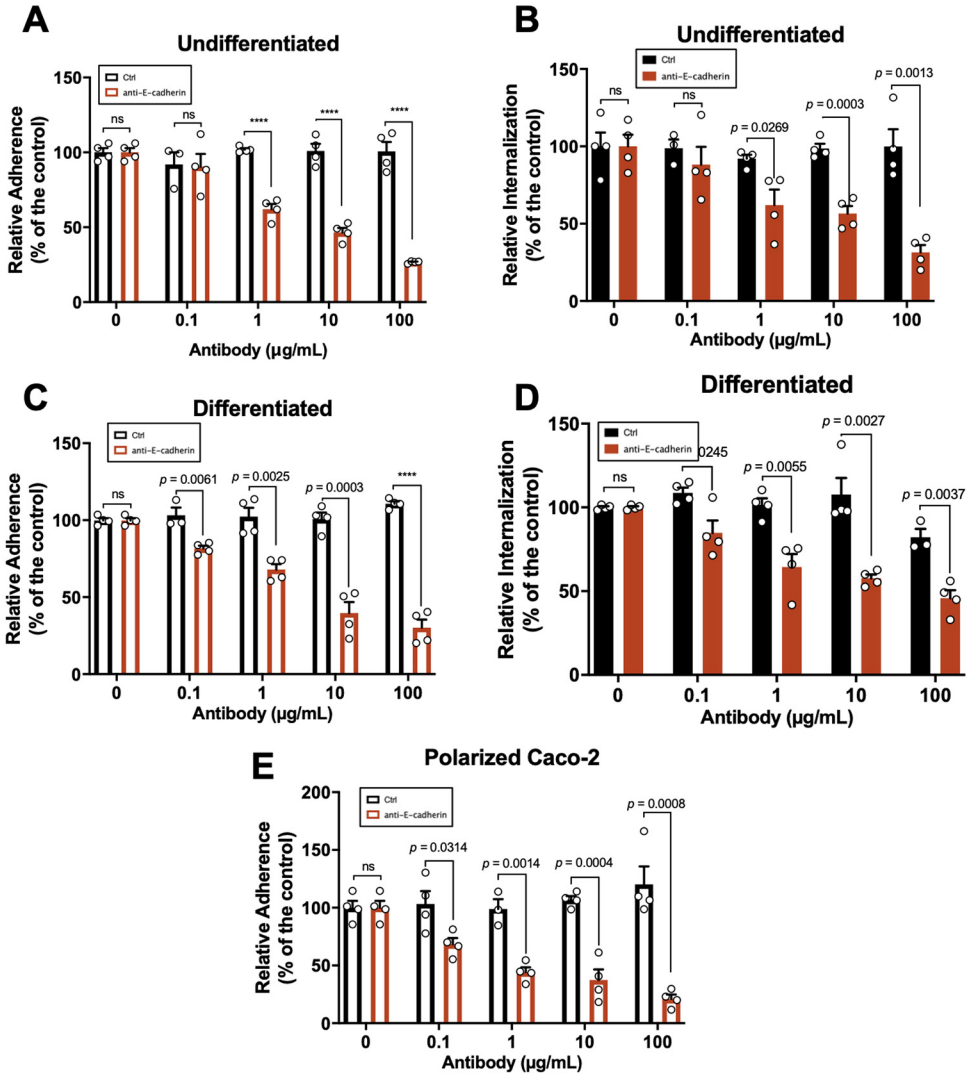

FIG 5 E-cadherin-blocking antibodies decrease the spore interaction with IECs. Undifferentiated, differentiated, and polarized Caco-2 cells were infected with *C. difficile* spores preincubated with FBS in the presence of anti-E-cadherin or nonimmune IgG as control (Ctrl) for 2 h at 37°C. (A and B) Adherence (A) and internalization (B) of *C. difficile* spores in undifferentiated Caco-2 cells. (C and D) Adherence (C) and internalization (D) in differentiated Caco-2 cells. (E) *C. difficile* spore adherence in polarized Caco-2 cells. Data showed in each panel are normalized to 0 μg mL^{-1} of antibody. The data are the mean of 6 independent wells collected in 2 independent experiments. In bars, each dot represents 1 independent well collected from 2 independent experiments. For each bar, a total of ~1,300 spores were analyzed. Error bars indicate mean ± SEM. Statistical analysis was performed by two-tailed unpaired Student's *t* test. ns, $P > 0.05$; ****, $P < 0.0001$.

was demonstrated by the dose-dependent binding. Additionally, we evaluated the distribution of binding of E-cadherin to the spore surface by immunofluorescence. Upon micrograph analysis, we observed that anti-E-cadherin-immunostained spores exhibited a nonhomogeneous fluorescence intensity surrounding the spore (Fig. 7B). In spores, the fluorescence intensities for E-cadherin were 156, 189, 258, 304, and 369% relative to the control upon incubation with 1, 2.5, 5, 10, and 25 μg mL^{-1} of E-cadherin (Fig. 7C). Next, based on the visual detection of fluorescence intensity (Fig. 7B), we established a fluorescence intensity cutoff limit for those *C. difficile* spores that were visually associated with 2.5 μg mL^{-1} E-cadherin. Based on this threshold, 59, 65, and 66% of the spores were positive for E-cadherin in the presence of 5, 10, and 25 μg mL^{-1} E-cadherin, respectively. Finally, we evaluated E-cadherin fluorescence intensity distribution for positive immunodetected spores, and we observed that they were mainly distributed between 1.4 and 2.1 normalized fluorescence intensity arbitrary

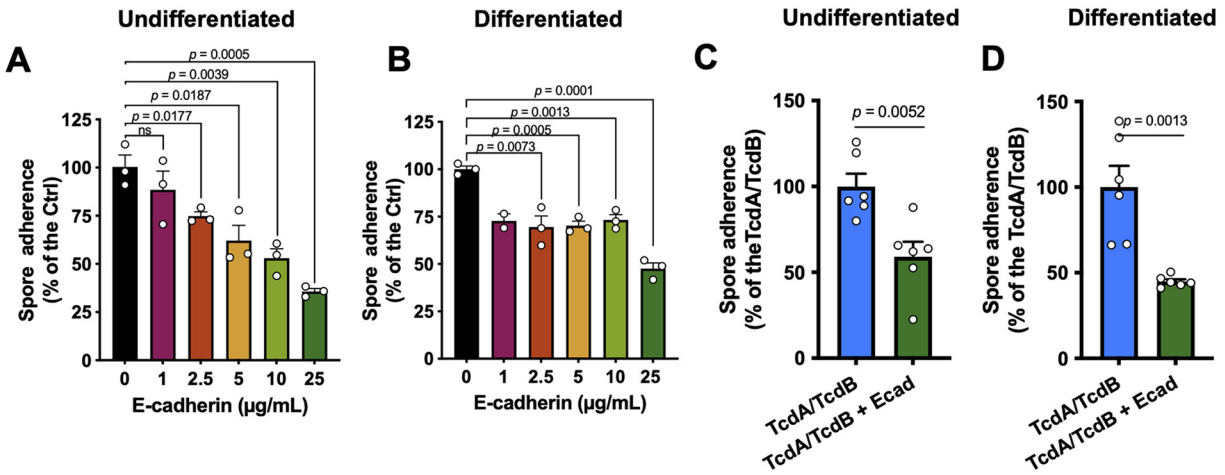

FIG 6 E-cadherin competitively reduces spore adherence to healthy and intoxicated IECs. (A and B) Undifferentiated (A) and differentiated (B) Caco-2 cells were infected for 3 h at an MOI of 10 with *C. difficile* spores pretreated with 1, 2.5, 5, 10, and 25 μg/mL of human purified E-cadherin, and adhered cells were identified and quantified as described in Materials and Methods. (C and D) TcdA- and TcdB-intoxicated undifferentiated (C) and differentiated (D) Caco-2 cells were infected for 3 h at an MOI of 10 with *C. difficile* spores pretreated with 25 μg/mL of human purified E-cadherin, and adhered cells were identified and quantified as described in Materials and Methods. Data are the mean of 6 independent wells collected in 2 independent experiments.

units (Fig. 7D). Taken together, these results indicate that E-cadherin ligand binding sites are nonhomogeneously distributed on the C. difficile spore surface, and E-cadherin binds in a concentration-dependent manner to *C. difficile* spores in a heterogeneous and skewed manner to *C. difficile* spores.

E-cadherin interacts with hairlike projections of *C. difficile* spores. The outermost structure of *C. difficile* spores are the hairlike projections, formed in part by BclA3, that are common in epidemically relevant strains (16, 20, 37). Isogenic sporulating cultures of *C. difficile* lead to the formation of spores with two exosporium morphotypes that exhibit hairlike projections, spores with a thick exosporium layer display distinctive electron-dense bumps, and spores with a thin exosporium lack these bumps (37–40), suggesting that this exosporium morphotype diversity might be contributing to E-cadherin spore-binding variability. Consequently, to gain ultrastructural insight into the spore-E-cadherin interaction, *C. difficile* spores incubated with E-cadherin and subsequently immunogold labeled for E-cadherin, were imaged by TEM. We observed E-cadherin-gold particles in close contact with the exosporium of *C. difficile* spores, particularly with the hairlike projections (Fig. 8A and B). No gold particles were observed in spores without the E-cadherin incubation (data not shown). Next, within the E-cadherin-positive spores, we observed gold particles in 52/236 (22.1%) of the spores (Fig. 8C). Of these, 19/52 (36.5%) and 33/52 (63.5%) of the E-cadherin-bound spores corresponded to spores with thin and thick exosporiums, respectively (Fig. 8D). These results are representative of a 90-nm slice of the sample, and therefore, the number of gold particles corresponds to those only present in the slice and not of a complete spore. These results suggest that E-cadherin binds preferentially to thick-exosporium layer spores, which seem to have enriched hairlike projections.

Most *C. difficile* genomes encode three collagen-like proteins of the BclA family of proteins (41). However, *C. difficile* strain R20291 only encodes two *bclA* orthologues (i.e., *bclA2* and *bclA3*) (41). Therefore, we reasoned to use previously characterized *bclA1*, *bclA2*, and *bclA3* mutants in strain 630 (42) to address by ELISA whether these collagen-like proteins could be implicated in E-cadherin binding to *C. difficile* spores. As with R20291 spores, E-cadherin binding to 630 spore-coated wells was evident (Fig. 8E). Notably, upon coating wells with spores of *bclA1*, *bclA2,* or *bclA3* mutants, a dose-dependent binding of E-cadherin to spore-coated wells was similar to that of wild-type spores, with the exception of *bclA3* mutant spores, which exhibited higher binding of E-cadherin (Fig. 8E). Overall, these results suggest the presence of an unidentified E-cadherin-specific spore surface ligand.

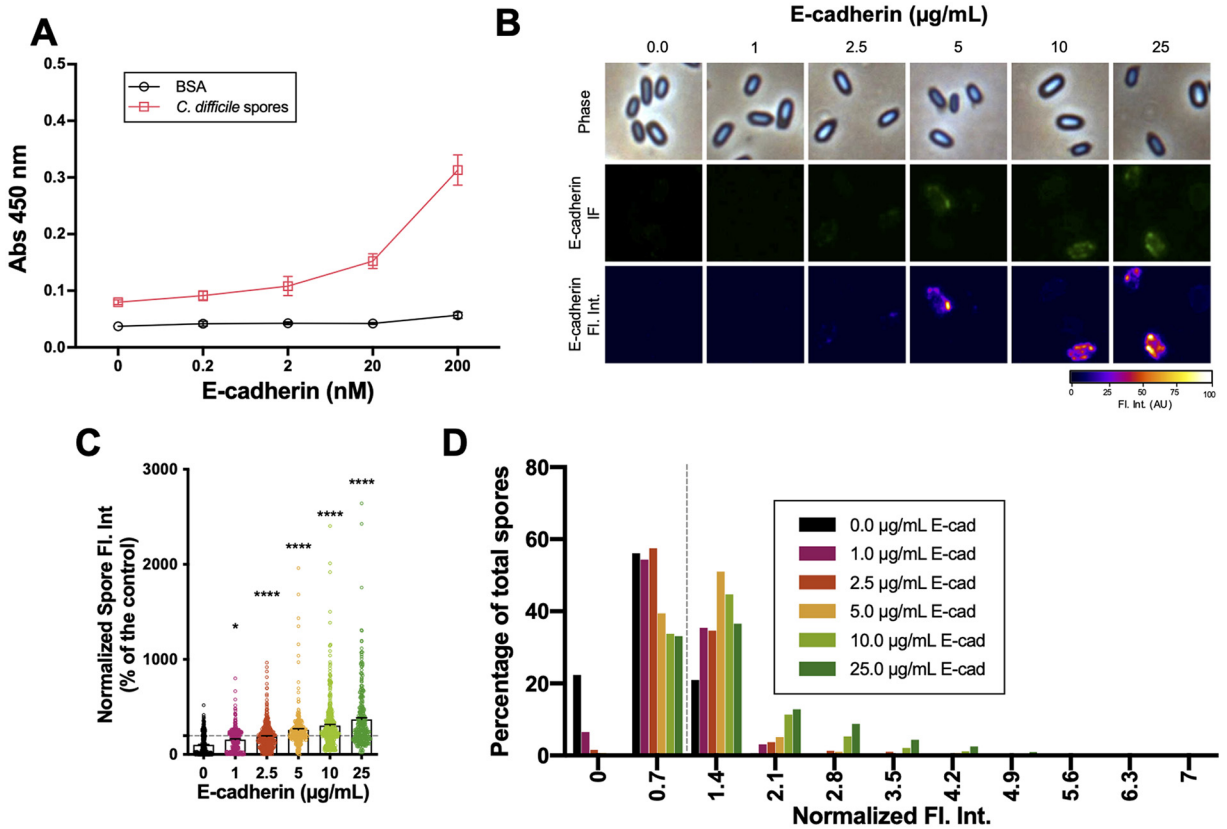

FIG 7 E-cadherin interacts with *C. difficile* spores. (A) Solid-phase binding assay of *C. difficile* R20291 spores or BSA as control with increasing concentrations (i.e., 0.2, 2.0, 20, and 200 nM) of human purified E-cadherin. The data represented are the mean of 9 independent wells collected in 3 independent experiments. (B) Representative phase-contrast micrograph, immunofluorescence against E-cadherin, and immunofluorescence plot profile of 4×10^7 *C. difficile* spores that were incubated with increasing concentrations (i.e., 1, 2.5, 5, 10, and 25 μg mL^{-1}) of human purified E-cadherin for 1 h at 37°C. (C) Quantitative analysis of fluorescence intensity. (D) Distribution of E-cadherin fluorescence intensity of *C. difficile* incubated with increasing concentrations (i.e., 1, 2.5, 5, 10, and 25 μg mL^{-1}) of human purified E-cadherin. A total of ~450 spores were analyzed for each condition. Error bars indicate mean ± SEM. Statistical analysis was performed by two-tailed unpaired Student's *t* test. *, $P < 0.05$; ****, $P < 0.0001$.

DISCUSSION

A major clinical challenge that remains unresolved is how to address the high rates of CDI recurrence (43–45). *C. difficile* spores are regarded as the key virulence factors required for recurrence and transmission of the disease (16, 17). Although significant work has advanced our understanding of the biology of *C. difficile* spores (16, 37), the mechanisms through which *C. difficile* spores interact with the host within the environment of the colon remain poorly described. The integrity of the intestinal epithelial barrier is key in preventing pathogen translocation (22). However, in the healthy intestinal mucosa, the apical and basolateral cell sides are not always separated. The adherens junctions, where E-cadherin is located, can be accessible in certain situations, i.e., along lateral membranes of goblet cells (20, 46, 47), extruding apoptotic sites, produced transiently when senescent cells are expelled and detached from the epithelium (46, 48, 49) and in epithelial folds of the intestinal villus produced by tension and constriction forces (46). In this context, we have demonstrated that E-cadherin is a novel spore adherence receptor that promotes binding of *C. difficile* spores at adherens junctions, and this binding is enhanced in intoxicated IECs.

Work by others has demonstrated that E-cadherin is hijacked by several pathogens, including *Listeria monocytogenes*, *Fusobacterium nucleatum*, and *Streptococcus pneumoniae* (23–26, 46). This report expands the list of pathogens that hijack E-cadherin for adherence and entry to include *C. difficile* spores. Our prior work demonstrated that *C. difficile* spores adhere to IECs *in vitro* (18) and gain entry into host cells via fibronectin and vitronectin in

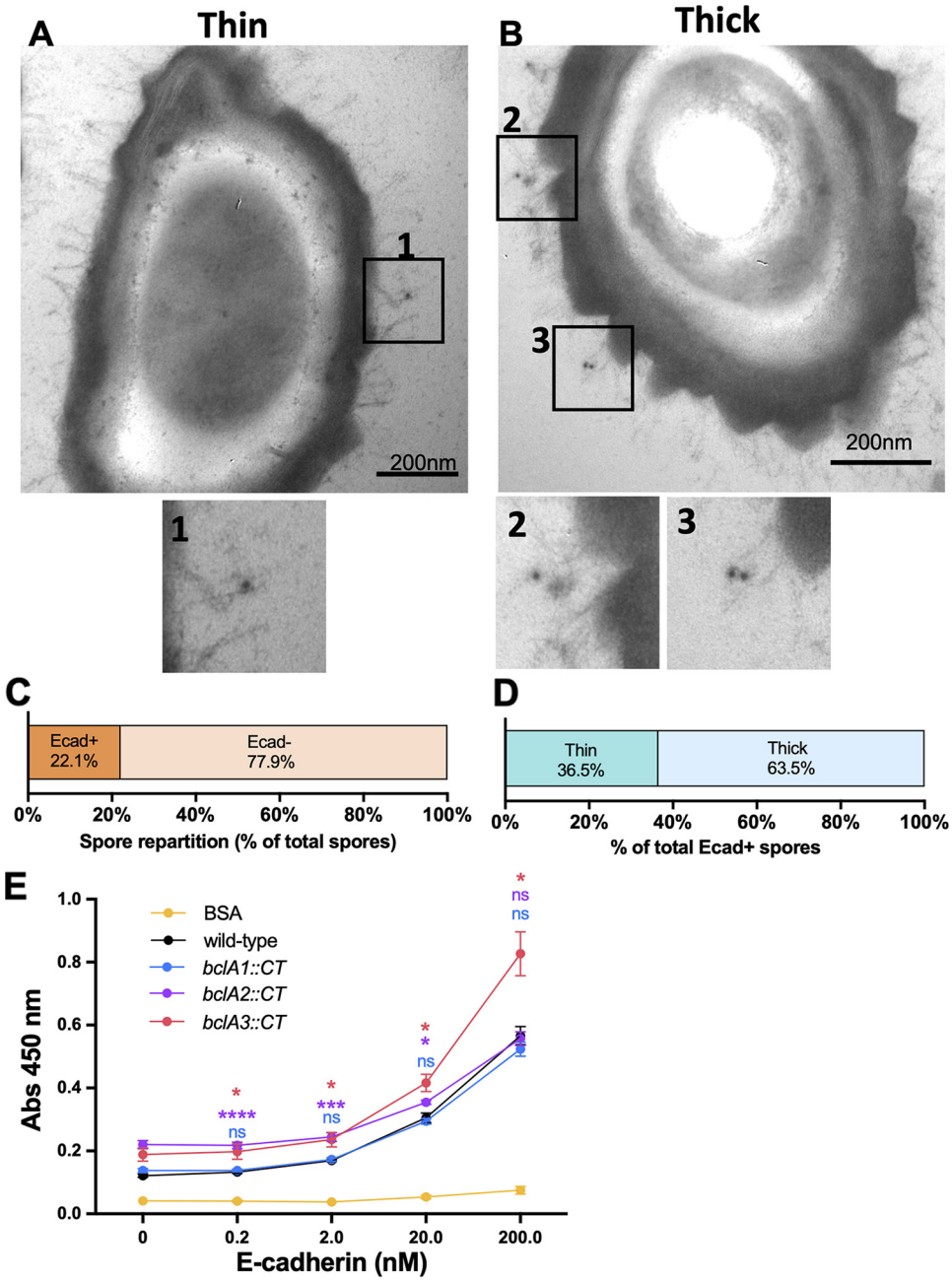

FIG 8 Immunoelectron microscopy of E-cadherin-gold complex binding to *C. difficile* spores. (A and B) TEM of *C. difficile* spores incubated with 10 μg mL^{-1} E-cadherin or without E-cadherin (negative control; data not shown). They were then incubated with anti-E-cadherin and anti-mouse–12-nm gold complex. Spores were stratified in thin and thick exosporium spores. Bottom panels are magnifications of the black squares highlighting immunogold spots and quantification of the *C. difficile* spores associated with E-cadherin. (C and D) Classification of E-cadherin-positively associated with *C. difficile* spores according to the morphology of the spore (C), thin or thick exosporium (D), represented as the percentage of the total E-cadherin-positive spores. Figures show representative spores with a thin or thick exosporium layer and are representative of 2 independent experiments. A total of 100 spores were quantified. (E) Solid-phase binding assay of human E-cadherin to *C. difficile* spores of 630 wild-type and isogenic mutant strains of *bclA1*, *bclA2*, and *bclA3* or BSA as a control with increasing concentrations (i.e., 0.2, 2.0, 20, and 200 nM) of human purified E-cadherin. The data represented are the mean of 9 independent wells collected in 3 independent experiments. Statistical analysis was performed by one-way analysis of variance (ANOVA) followed by Bonferroni's correction for multicomparisons. ns, $P > 0.05$; *, $P < 0.05$, $P < 0.001$; ****, $P < 0.0001$. Colors indicating significance correspond to the mutant strain being compared to wild type.

an integrin-dependent pathway (20). The ~70 to 80% reduction in adherence in undifferentiated, differentiated, and polarized monolayers of Caco-2 cells upon blockade with anti-E-cadherin antibodies or competition with purified E-cadherin suggests that E-cadherin is a major cellular adherence receptor for *C. difficile* spores. Fibronectin, vitronectin, and integrin receptors are typically located in the basolateral membrane (36, 50–53), where E-cadherin is localized. However, whether additional cellular junction proteins also act as receptors and/or promote spore entry remains unclear. An outstanding question is whether E-cadherin acts as an anchoring protein allowing *C. difficile* spores to bind fibronectin/vitronectin and their cognate integrins to trigger internalization or whether spore binding to E-cadherin alone is capable of triggering a signal for internalization of *C. difficile* spores. This question will be addressed in future studies.

Another conclusion of this work is that *C. difficile* spores bind to E-cadherin in a dose-dependent manner. *L. monocytogenes* interacts with human and not with mouse E-cadherin through InlA (26). While the exosporium of *C. difficile* spores has no orthologs of InlA (54), we show E-cadherin binding to the hairlike projections of the exosporium. *C. difficile* spores form two exosporium morphotypes during sporulation (i.e., a thick and a thin exosporium layer) (37); among the main differences is the presence of electron-dense bumps underlying the hairlike projections. Whether there are differences in the hairlike projections and in their numbers between both morphotypes, is unclear and a matter of study in our laboratory. Notably, spores of *bclA1* and *bclA2* mutants in strain 630 were able to bind to E-cadherin to a similar extent as wild-type spores, suggesting redundance in function. It was surprising to observe that *bclA3* mutant spores bind higher levels of E-cadherin, suggesting that absence of BclA3 might uncover an alternative spore surface ligand(s) implicated in binding of E-cadherin to the spore surface. Current ongoing work in our laboratory aims to identify the spore surface ligand(s) that bind to E-cadherin and its implication in disease.

A final and major conclusion of this work is that TcdA and TcdB intoxication increases spore adherence to IECs in an E-cadherin-specific manner. This is supported by increased association between basolateral E-cadherin and *C. difficile* spores and by the observation that soluble E-cadherin can reduce the adherence of *C. difficile* spores to TcdA- and TcdB-intoxicated IECs. *C. difficile* toxins TcdA and TcdB cause a disruption of the cell-cell junctions (10, 12, 13), causing a loss of cellular polarity (9–11). This disruption is caused by a dissociation of tight and adherens junction proteins. In this context, our work contributes to understanding how *C. difficile* spores interact with TcdA- and TcdB-intoxicated IECs. Our results demonstrate that differentiated TcdA- and TcdB-intoxicated monolayers show an increased accessibility of E-cadherin that correlates with an increase in spore adherence to TcdA- and TcdB-intoxicated cells. These observations suggest that during CDI, TcdA and TcdB increase the E-cadherin accessibility, contributing to spore adherence and entry into the IECs *in vivo*. Indeed, since intracellular *C. difficile* spores contribute to disease recurrence (20), TcdA and TcdB intoxication may significantly contribute to *C. difficile* spore adherence and internalization during CDI, contributing overall to disease recurrence. These hypotheses are in agreement with clinical observations in CDI patients where high titers of endogenous antibodies against the *C. difficile* toxins correlate with reduced R-CDI rates (55) and with the reduced R-CDI observed in the clinical trials of bezlotoxumab (15). The development of multifactorial treatment with intervention in TcdA and TcdB, spore adherence, and entry to IECs might, importantly, reduce the R-CDI rates.

MATERIALS AND METHODS

Bacterial growth conditions. *C. difficile* was grown under anaerobic conditions at 37°C in a Bactron III-2 chamber (Shellab, OR, USA) in BHIS medium (3.7% brain heart infusion broth [BD, USA] supplemented with 0.5% of yeast extract [BD, USA], and 0.1% L-cysteine [Merck, USA] liquid or on plates with 1.5% agar [BD, USA]). *C. difficile* R20291 wild-type B1/NAP1/PCR-ribotype 027 was obtained from CRG0825 stock at Nottingham Clostridia Research Group (56). *C. difficile* 630Δ*erm* is a toxigenic (*tcdA*$^+$ *tcdB*$^+$) strain of *C. difficile* isolates from a patient with pseudomembranous colitis during an outbreak of CDI (57). *C. difficile* 630Δ*erm* clostron mutant strains *bclA1::CT*, 630Δ*erm bclA2::CT*, and 630Δ*erm bclA3::CT* have insertional inactivated alleles encoding for the exosporium collagen-like proteins BclA1, BclA2, and BclA3, respectively (42), and were a kind gift from Simon Cutting (School of Biological Sciences, Royal

Holloway, University of London). *Bacillus megaterium* transformed with the plasmid pHIS 1622 that contains the cloned genes *tcdA* and *tcdB* of *C. difficile* VPI 10463 (58) was aerobically grown at 37°C in Luria-Bertani (BD) with 10 μg/mL tetracycline.

Cell lines and culture conditions. Caco-2 cells (ATCC, USA) were grown at 37°C with 5% CO_2 with Dulbecco's modified Eagle's minimal essential medium high glucose (DMEM; HyClone, USA) supplemented with 10% fetal bovine serum (FBS; HyClone, USA), 50 U mL^{-1} penicillin, and 50 μg mL^{-1} streptomycin (Corning Cellgro, USA) as previously described For experiments, cells were plated over glass coverslips in 24-well plates and were cultured for 2 days postconfluence (undifferentiated) or 8 days postconfluence (differentiated), changing the media every other day. To polarize, Caco-2 cells were cultured onto 12 mm Transwell plates (Corning, USA) with a pore size of 0.4 μm until transepithelial electric resistance was $>250\ \Omega \times cm^2$.

Recombinant *C. difficile* toxin purification. *C. difficile* toxins TcdA and TcdB were expressed in *B. megaterium* transformed with the plasmid pHIS1622, containing the cloned genes *tcdA* and *tcdB* of *C. difficile* VPI 10463 as previously described (58). Briefly, transformed *B. megaterium* was cultured in Luria-Bertani medium (BD, USA) supplemented with 10 μg mL^{-1} tetracycline, and 35 mL of an overnight culture was used to inoculate 1 L of media. Bacteria were grown at 37°C with 220 rpm. Toxin expression was induced with 0.5% D-xylose once the culture reached an optical density at 600 nm (OD_{600}) of 0.5. Cells were harvested after 4 h by centrifugation at 4,750 $\times$ *g* and resuspended in 200 mL of binding buffer (20 mM Tris [pH 8.0] and100 mM NaCl for TcdA and 20 mM Tris [pH 8.0] and 500 mM NaCl for TcdB) supplemented with 0.16 μg mL^{-1} DNase, 10 mg mL^{-1} lysozyme, and protease inhibitors (catalog no. P8849; Sigma). Cell lysis was performed using an Emulsiflex homogenizer, and lysates were centrifuged at 48,000 $\times$ *g* for 30 min. The toxins were purified from the supernatant by nickel affinity, anion exchange, and size-exclusion chromatography. Toxins were eluted and stored in 20 mM HEPES (pH 7.0) and 50 mM NaCl.

Spore preparation and purification. *C. difficile* spores were purified as we previously described (28). Briefly, *C. difficile* spores were cultured overnight in BHI medium in a Bactron III-2 anaerobic chamber. Then, a 1:500 dilution was plated in TY agar plates (3% Trypticase soy, 0.5% yeast extract, and 1.5% Bacto agar [BD, USA]) and incubated for 7 days at 37°C in anaerobiosis. Colonies were harvested with sterile, cold Milli-Q water, washed 3 times, and purified with 50% Nycodenz. The spore suspension was 99% free of vegetative cells, sporulating cells, and debris. Spores were quantified in a Neubauer chamber and stored at −80°C until use.

Immunofluorescence of cell monolayers. To evaluate E-cadherin distribution in undifferentiated and differentiated Caco-2 cells, cells were washed with phosphate-buffered saline (PBS) and were fixed with PBS-4% paraformaldehyde for 20 min at 4°C and blocked with PBS-3% BSA 1 h at room temperature (RT). To stain the accessible E-cadherin, cells were incubated with 1:50 of primary antibody mouse polyclonal anti-human E-cadherin (catalog no. sc-8426; Santa Cruz Biotechnology, USA) in PBS-3% BSA for 2 h at RT followed by two washes with PBS and 1:200 secondary antibody, donkey anti-mouse Alexa Fluor 568 (catalog no. ab175700; Abcam, USA). To detect the total E-cadherin, fixed samples were permeabilized with PBS-0.2% Triton 100-X for 10 min at RT and blocked with PBS-3% BSA for 1 h at RT. The total protein was detected with the same primary antibody used for accessible E-cadherin; primary antibody mouse polyclonal anti-human E-cadherin in PBS-3% BSA that was incubated for 2 h at RT and then was washed and incubated with 1:200 secondary antibody donkey anti-mouse Alexa Fluor 568. The nonpermeabilized samples stained for accessible E-cadherin were permeabilized with PBS-0.2% Triton 100-X for 10 min at RT and washed, and to stain the F-actin, cells were incubated with 1:1,000 Phalloidin iFluor 488 (catalog no. ab176753; Abcam, USA) in PBS for 30 min at RT. Cells were washed, and nuclei were stained with 8 μg mL^{-1} Hoechst 33342 (Thermo Fisher, USA) in PBS for 10 min at RT. Then samples were washed and mounted using Dako fluorescent mounting medium (Dako, Denmark). Samples were visualized in the confocal microscope Leica TCS LSI (Leica, Germany). Please see below.

To study the redistribution of E-cadherin in TcdA- and TcdB-intoxicated cells, differentiated Caco-2 cells cultured into 24-well plates were washed twice with Dulbecco's phosphate-buffered saline (DPBS) (HyClone, USA) and intoxicated with 600 pM TcdA and 600 pM TcdB for 3, 6, and 8 h in DMEM without serum. As a control, cells were incubated in the same solution without TcdA and TcdB. Then, cells were rinsed with PBS, fixed with PBS-4% paraformaldehyde, washed with PBS, and blocked with PBS-1% BSA at 4°C overnight. To stain the surface, accessible E-cadherin cells were incubated with 1:200 of the mouse monoclonal antibody (MAb) anti-E-cadherin for 1 h at RT, washed, and followed with incubation with 1:400 donkey anti-mouse IgG, Alexa Fluor 488 (catalog no. ab150109; Abcam, USA) for 1 h at RT. To detect the total protein, samples were permeabilized with PBS-0.2% Triton 100-X for 10 min at RT and blocked with PBS-1% BSA for 1 h at RT. The total protein was detected with the same primary antibody used before, washed, and samples were incubated with donkey anti-mouse IgG Alexa Fluor 568. Samples were mounted using Dako fluorescent mounting medium and were visualized in the confocal microscope Leica Sp8 (Leica, Germany; please see below).

To evaluate *C. difficile* spore association with accessible E-cadherin in TcdA- and TcdB-intoxicated IECs, differentiated Caco-2 cells were intoxicated with 600 pM TcdA and 600 pM TcdB for 8 h at RT as described above. Then cells were infected with *C. difficile* spores at a multiplicity of infection (MOI) of 10 for 1 h at 37°C. Then cells were washed, fixed with PBS-4% paraformaldehyde for 10 min at RT, and blocked with PBS-1% BSA overnight at 4°C, and *C. difficile* spores were stained with 1:1,000 primary polyclonal anti-*C. difficile* spore IgY batch 7246 antibodies (29) (Aves Labs, USA) in PBS-1% BSA for 1 h at RT. Following two PBS washes, samples were incubated with 1:400 goat anti-chicken IgY secondary antibodies Alexa Fluor 488 (catalog no. ab150173; Abcam, USA) in PBS-3% BSA for 1 h at RT and washed two times with PBS, and accessible E-cadherin was stained as described above. Cellular nuclei were stained with 8 μg mL^{-1} Hoechst 33342 for 15 min at RT. Finally, samples were mounted and analyzed by confocal microscopy using a Leica SP8.

The Leica microscopes TCS LSI and SP8 at the Confocal Microscopy Core Facility of the Universidad Andrés Bello were used. To evaluate E-cadherin distribution in undifferentiated and differentiated Caco-2 cells, Leica TCS LSI was used with 63× ACS APO oil objective (numerical aperture, 1.3), with an optical zoom of 2×. Micrographs were acquired using excitation wavelengths of 405, 488, and 532 nm, and signals were detected with an photomultipliers (PMT) spectral detector (430 to 750 nm). Emitted fluorescence was splitted into four detection channels (SP8 standard PMTs) with a Quadband Dichroic (405, 488, 561, and 635 nm). Images of 1,024 by 1,024 pixels were acquired every 0.3 μm. To observe the redistribution of accessible E-cadherin and total E-cadherin in TcdA- and TcdB-intoxicated cells, a Leica SP8 was used with HPL APO CS2 40× oil immersion (numerical aperture, 1.30). For signal detection, three PMT spectral detectors were used, PMT1 (410 to 483) DAPI (4′,6-diamidino-2-phenylindole); PMT2 (505 to 550), Alexa Fluor 488; and PMT3 (587 to 726), Alexa Fluor 555. Emitted fluorescence was split with dichroic mirrors DD488/552. Pictures that were 1,024 by 1,024 pixels were captured every 0.3 μm. Images of three-dimensional (3D) reconstructions of the Caco-2 monolayers were created using ImageJ software (NIH, USA). In undifferentiated and differentiated cells, accessible E-cadherin cells were quantified as the number of cells with positive staining. To quantify the redistribution of E-cadherin, the fluorescence intensity of each slide was measured using the plug-in "Measure Stack" of Fiji (ImageJ), and the sum of the fluorescence intensity of each slide is considered the fluorescence intensity of the z-stack of a field for accessible and total E-cadherin. For each field, the same number of slides was used.

Quantification of *C. difficile* spore adherence and internalization. To evaluate spore adherence and internalization in TcdA- and TcdB-intoxicated cells, differentiated Caco-2 cells were incubated with 600 pM TcdA and 600 pM TcdB for 8 h in DMEM without serum. As a control, cells were incubated in the same solution without TcdA and TcdB, or cells were incubated with TcdA and TcdB, which were previously heat inactivated at 70°C for 5 min. Then, undifferentiated and differentiated Caco-2 cells were infected with *C. difficile* spores at an MOI of 10 for 3 and 1 h at 37°C, respectively. Unbound spores were rinsed off with PBS, cells were fixed with PBS-4% paraformaldehyde for 10 min, and adhered spores were stained as described below.

To evaluate spore adherence and entry in the presence of anti-E-cadherin, undifferentiated, differentiated, and polarized Caco-2 cells were incubated with 0.1, 1.0, 10, or 100 μg mL^{-1} of mouse monoclonal anti-human E-cadherin or, as control, nonimmune IgG antibody of rabbit serum (catalog no. I5006; Sigma-Aldrich, USA) for 2 h at 37°C. Then, cells were infected for 3 h at 37°C with *C. difficile* spores, which were previously incubated with 20 μL of FBS per well for 1 h at 37°C. Cells were washed two times with PBS to remove unbound spores and were fixed with PBS-4% paraformaldehyde for 10 min at RT, and adhered spores were stained as described below.

To evaluate spore adherence and entry in the presence of purified E-cadherin, undifferentiated and differentiated Caco-2 cells were infected with *C. difficile* spores previously incubated with 1, 2.5, 5, 10, and 25 μg mL^{-1} of human purified E-cadherin (catalog no. 5085; Sigma-Aldrich, USA) in DMEM or DMEM without FBS as control for 1 h at 37°C. Then, cells were infected with spores and incubated for 3 h at 37°C. Cells were washed two times with PBS to remove unbound spores and fixed with PBS-4% paraformaldehyde for 10 min at RT, and adhered spores were stained as described below.

To evaluate whether the presence of E-cadherin decreases the spore adherence in TcdA- and TcdB-intoxicated cells, undifferentiated and differentiated Caco-2 cells were 8-h TcdA and TcdB intoxicated and were infected for 1 h at 37°C with *C. difficile* spores previously incubated with 25 μg mL^{-1} of E-cadherin for 1 h at 37°C. Cells were washed two times with PBS to remove unbound spores and fixed with PBS-4% paraformaldehyde for 10 min at RT, and adhered spores were stained as described below.

In undifferentiated, differentiated, and polarized *C. difficile* spore-infected Caco-2 cells, adhered *C. difficile* spores were immunostained using the intracellular spore exclusion immunostaining assay as previously described (20). For this, *C. difficile* spore-infected cells were washed three times with PBS at RT and blocked with PBS-3% BSA overnight at 4°C, and samples were incubated with anti-*C. difficile* spore goat serum 1:50 (purchase order number PAC 5573; Pacific Immunology, USA) in PBS-1% BSA for 1 h at RT. The cells were washed 3 times with PBS and incubated with 1:400 secondary antibody donkey IgG anti-goat CFL 488 (catalog no. sc-362255; Santa Cruz Biotechnology, USA) for 1 h at RT. Cells were washed, and DNA was stained with 8 μg mL^{-1} Hoechst 33342 for 15 min at RT. In the case of polarized cells, to stain the F-actin, samples were incubated with 1:100 Phalloidin Alexa Fluor 568 (catalog no. A12380; Invitrogen, USA) for 30 min at RT. Samples were washed three times with PBS and one time with distilled water and mounted with Dako fluorescent mounting medium. Samples were visualized in the epifluorescence microscope Olympus BX53 with UPLFLN 100× oil objective (numerical aperture, 1.30). Images were captured with the camera for fluorescence imaging, QImaging R6 Retiga, and pictures were analyzed with ImageJ. Adhered spores were considered spores in phase contrast that were marked in fluorescence. Internalized spores were considered spores in phase contrast but do not have fluorescence. In the case of polarized cells, it was only possible to quantify adhered spores. The numbers of adhered spores were quantified, and data were normalized to the control.

ELISA of E-cadherin bound to *C. difficile* spores. Ninety-six-well plates were coated overnight at 4°C with 100 μL/well containing 1.6× 10^8 spores mL^{-1} or with 100 μL of PBS containing 1 μg of BSA in PBS (as a control) overnight at 4°C. Wells were washed 5 times with PBS-0.05% Tween 20 (PBS-Tween) to remove unbound spores and blocked with 200 μL of PBS-Tween-2% BSA (Sigma-Aldrich, USA) for 1 h at 37°C. The spores were washed and incubated with 50 μL of 0.2, 2.0, 20, and 200 nM recombinant human purified E-cadherin for 1 h at 37°C. Unbonded E-cadherin was washed 5 times with 150 μL PBS-Tween and was incubated with 50 μL of 1:50 IgG of mouse anti-E-cadherin in PBS-Tween-1% BSA for 1 h at 37°C. Wells were washed five times with PBS-Tween and then incubated with 50 μL of 1: 5,000 secondary antibody anti-mouse horseradish peroxidase (HRP; catalog no. 610-1302, Rockland, USA) 1 h at 37°C.

Then, wells were washed five times with PBS-Tween and once with carbonate buffer (pH 9.6). Finally, wells were incubated with 50 μL of buffer substrate (17 mM citric acid, 65 mM potassium phosphate, 0.15% hydrogen peroxide, and 0.4% *O*-phenylenediamine) for 20 min at RT. The reaction was stopped with 25 μL of 4.5 N H_2SO_4. The color intensity was quantified at 450 nm using the plate reader Infinite F50 (Tecan, Switzerland).

Immunofluorescence of E-cadherin bound to *C. difficile* spores. The immunofluorescence was performed as previously described with modification (19). Briefly, 4×10^7 *C. difficile* spores were incubated with 1, 2.5, 5.0, 10, and 25 μg mL^{-1} of recombinant human purified E-cadherin in PBS for 1 h at 37°C. Spores were washed 5 times with PBS and fixed with PBS-4% paraformaldehyde in poly-L-lysine-treated 12-mm glass coverslips (Paul Marienfeld GmbH, Germany). The spores were washed 3 times with PBS and blocked with PBS-3% BSA for 1 h at RT. Then, samples were incubated with 1:50 mouse IgG anti-E-cadherin for 2 h at RT and washed 3 times with PBS and once with distilled H_2O. Finally, samples were mounted with Dako fluorescent mounting medium, and images were captured in an epifluorescence microscope, Olympus BX53. The fluorescence intensity was quantified using Fiji (ImageJ). Data were normalized as $(\text{fluorescence intensity/area})_{\text{sample}} - (\text{fluorescence intensity/area})_{\text{background}}$. The Surface Plot was generated with the plug-in 3D surface plot of Fiji.

SDS-PAGE and Western blot analysis of intoxicated Caco-2 cells. Undifferentiated and differentiated Caco-2 cells were intoxicated for 3, 6, and 8 h with TcdA and TcdB in 24-well plates. The cells were washed and frozen at −80°C. The frozen cells were lysed with 80 μL/well of cold radioimmunoprecipitation assay (RIPA) buffer (50 mM Tris-HCl, 150 mM NaCl, 0.5% deoxycholate, 1% NPO_4, 1 mM EGTA, 1 mM EDTA, 0.5% SDS, and protease inhibitor) in ice and centrifuged at 18,400 $\times$ *g* for 15 min at 4°C. The supernatant was collected, and 20 μg of protein was suspended in 2$\times$ SDS-PAGE sample loading buffer, boiled, and electrophoresed on 12% and 4% acrylamide SDS-PAGE gels. Proteins were transferred to nitrocellulose membrane and blocked with 5% nonfat milk in Tris-buffered saline (TBS) for 1 h at RT. Membranes were probed for nonglucosylated Rac1 in TBS containing 0.1% Tween (TTBS) with 5% milk and 1:1,000 mouse anti-Rac1 (clone 102/Rac1 610650; BD Bioscience, USA) and then incubated overnight at RT and for 6 h at RT. The membranes were washed with TTBS and incubated with 1:5,000 goat anti-mouse HRP for 1 h at RT in 5% milk-TTBS. Samples were washed 3 times with TTBS, and HRP activity was detected with a chemiluminescence detection system (LI-COR) using PicoMax sensitive chemiluminescence HRP substrate (Bio-Rad, USA). To detect total Rac-1 in undifferentiated cells, membranes were incubated twice with mild stripping solution (1.5% glycine, 0.1% SDS, and 1% Tween 20, pH 2.2) for 7 min at RT, washed twice with PBS and twice with TTBS 0.05%, and blocked with 5% nonfat milk-TBS for 1 h at RT. For differentiated cells, total Rac1 was detected in the other membrane loaded simultaneously with the same concentration of protein. Membranes were incubated with 1:1,000 mouse anti-Rac1 (clone 23A8 05-389; MerckMillipore, USA) overnight at 4°C and 3 h at RT and then washed 3 times with TTBS. Membranes were then incubated with 1:5,000 goat anti-mouse HRP for 1 h at RT and washed 3 times with TTBS. HRP activity was detected using Li-Cor as described for nonglucosylated Rac1.

Transmission electron microscopy of E-cadherin bound to *C. difficile* spores. We incubated 2.5×10^8 *C. difficile* spores with 10 μg mL^{-1} of recombinant human-purified E-cadherin with PBS for 1 h at 37°C. Spores were washed 5 times with PBS and centrifugation at 18,400 $\times$ *g* for 5 min and were blocked with PBS-1% BSA for 20 min at RT. Then, samples were incubated with 1:50 IgG of mouse anti-E-cadherin in PBS-1% BSA for 1 h at RT and washed 3 times by centrifugation at 18,400 $\times$ *g* for 5 min with PBS. Spores were incubated with IgG anti-mouse conjugated to 10-nm gold nanoparticles (catalog no. G7777; Sigma-Aldrich, USA) for 1 h at RT. Then, they were washed 3 times with PBS-0.1% BSA by centrifugation at 18,400 $\times$ *g* for 5 min. Subsequently, spores were processed for TEM as previously described (19). Briefly, spores were fixed in 0.1 M cacodylate buffer-2.5% glutaraldehyde with 1% paraformaldehyde and then fixed with 0.1 M cacodylate buffer-1% osmium tetroxide and stained with 1% tannic acid for 30 min. Samples were dehydrated with increasing acetone concentrations as follows: 30% acetone (with 2% uranyl acetate only in this step) for 30 min, 50% acetone for 30 min, 70% acetone overnight, 90% acetone for 30 min, and 2 times with 100% acetone. Dehydrated samples were embedded in resin/acetone at a ratio of 3:1, 1:1, and 1:3 for 40 min each. Finally, samples were resuspended in resin for 4 h and incubated for 12 h at 65°C. With a microtome, 90-nm sections were cut and placed in a carbon-coated grid for negative staining and double staining with 2% uranyl acetate with lead citrate. Sections were observed in a transmission electron microscope, Phillip Tecnai 12 bioTwin of the Pontificia Universidad Católica de Chile. The distribution of thin or thick exosporium was quantified according to previously described morphotypes (38).

ACKNOWLEDGMENTS

This work was funded by FONDECYT regular 1191601, Millennium Science Initiative Program no. NCN17_093, and startup funds from the Department of Biology at Texas A&M University to D.P.-S. Additional funding support to P.C.-C. was from ANID-PCHA/Doctorado Nacional/2016-21161395.

We declare that we have no conflict of interest.

REFERENCES

1. Redelings MD, Sorvillo F, Mascola L. 2007. Increase in *Clostridium difficile*–related mortality rates, United States, 1999-2004. Emerg Infect Dis 13:1417–1419. https://doi.org/10.3201/eid1309.061116.
2. Stevens VW, Nelson RE, Schwab-Daugherty EM, Khader K, Jones MM, Brown KA, Greene T, Croft LD, Neuhauser M, Glassman P, Goetz MB, Samore MH, Rubin MA. 2017. Comparative effectiveness of vancomycin

and metronidazole for the prevention of recurrence and death in patients with *Clostridium difficile* infection. JAMA Intern Med 177:546–553. https://doi.org/10.1001/jamainternmed.2016.9045.
3. Di X, Bai N, Zhang X, Liu B, Ni W, Wang J, Wang K, Liang B, Liu Y, Wang R. 2015. A meta-analysis of metronidazole and vancomycin for the treatment of *Clostridium difficile* infection, stratified by disease severity. Braz J Infect Dis 19:339–349. https://doi.org/10.1016/j.bjid.2015.03.006.
4. Lyerly DM, Lockwood DE, Richardson SH, Wilkins TD. 1982. Biological activities of toxins A and B of *Clostridium difficile*. Infect Immun 35:1147–1150. https://doi.org/10.1128/iai.35.3.1147-1150.1982.
5. Lyras D, O'Connor JR, Howarth PM, Sambol SP, Carter GP, Phumoonna T, Poon R, Adams V, Vedantam G, Johnson S, Gerding DN, Rood JI. 2009. Toxin B is essential for virulence of *Clostridium difficile*. Nature 458:1176–1179. https://doi.org/10.1038/nature07822.
6. Kuehne SA, Cartman ST, Heap JT, Kelly ML, Cockayne A, Minton NP. 2010. The role of toxin A and toxin B in *Clostridium difficile* infection. Nature 467:711–713. https://doi.org/10.1038/nature09397.
7. Just I, Selzer J, Wilm M, von Eichel-Streiber C, Mann M, Aktories K. 1995. Glucosylation of Rho proteins by *Clostridium difficile* toxin B. Nature 375:500–503. https://doi.org/10.1038/375500a0.
8. Just I, Wilm M, Selzer J, Rex G, von Eichel-Streiber C, Mann M, Aktories K. 1995. The enterotoxin from *Clostridium difficile* (ToxA) monoglucosylates the Rho proteins. J Biol Chem 270:13932–13936. https://doi.org/10.1074/jbc.270.23.13932.
9. Nusrat A, von Eichel-Streiber C, Turner JR, Verkade P, Madara JL, Parkos CA. 2001. *Clostridium difficile* toxins disrupt epithelial barrier function by altering membrane microdomain localization of tight junction proteins. Infect Immun 69:1329–1336. https://doi.org/10.1128/IAI.69.3.1329-1336.2001.
10. Mileto SJ, Jardé T, Childress KO, Jensen JL, Rogers AP, Kerr G, Hutton ML, Sheedlo MJ, Bloch SC, Shupe JA, Horvay K, Flores T, Engel R, Wilkins S, McMurrick PJ, Lacy DB, Abud HE, Lyras D. 2020. *Clostridioides difficile* infection damages colonic stem cells via TcdB, impairing epithelial repair and recovery from disease. Proc Natl Acad Sci U S A 117:8064–8073. https://doi.org/10.1073/pnas.1915255117.
11. Kasendra M, Barrile R, Leuzzi R, Soriani M. 2014. *Clostridium difficile* toxins facilitate bacterial colonization by modulating the fence and gate function of colonic epithelium. J Infect Dis 209:1095–1104. https://doi.org/10.1093/infdis/jit617.
12. Hecht G, Pothoulakis C, LaMont JT, Madara JL. 1988. *Clostridium difficile* toxin A perturbs cytoskeletal structure and tight junction permeability of cultured human intestinal epithelial monolayers. J Clin Invest 82:1516–1524. https://doi.org/10.1172/JCI113760.
13. Hecht G, Koutsouris A, Pothoulakis C, LaMont JT, Madara JL. 1992. *Clostridium difficile* toxin B disrupts the barrier function of T84 monolayers. Gastroenterology 102:416–423. https://doi.org/10.1016/0016-5085(92)90085-d.
14. Leslie JL, Huang S, Opp JS, Nagy MS, Kobayashi M, Young VB, Spence JR. 2015. Persistence and toxin production by *Clostridium difficile* within human intestinal organoids result in disruption of epithelial paracellular barrier function. Infect Immun 83:138–145. https://doi.org/10.1128/IAI.02561-14.
15. Wilcox MH, Gerding DN, Poxton IR, Kelly C, Nathan R, Birch T, Cornely OA, Rahav G, Bouza E, Lee C, Jenkin G, Jensen W, Kim YS, Yoshida J, Gabryelski L, Pedley A, Eves K, Tipping R, Guris D, Kartsonis N, Dorr MB, MODIFY I and MODIFY II Investigators. 2017. Bezlotoxumab for prevention of recurrent *Clostridium difficile* infection. N Engl J Med 376:305–317. https://doi.org/10.1056/NEJMoa1602615.
16. Paredes-Sabja D, Shen A, Sorg JA. 2014. *Clostridium difficile* spore biology: sporulation, germination, and spore structural proteins. Trends Microbiol 22:406–416. https://doi.org/10.1016/j.tim.2014.04.003.
17. Deakin LJ, Clare S, Fagan RP, Dawson LF, Pickard DJ, West MR, Wren BW, Fairweather NF, Dougan G, Lawley TD. 2012. The *Clostridium difficile spo0A* gene is a persistence and transmission factor. Infect Immun 80:2704–2711. https://doi.org/10.1128/IAI.00147-12.
18. Paredes-Sabja D, Sarker MR. 2012. Adherence of *Clostridium difficile* spores to Caco-2 cells in culture. J Med Microbiol 61:1208–1218. https://doi.org/10.1099/jmm.0.043687-0.
19. Mora-Uribe P, Miranda-Cardenas C, Castro-Cordova P, Gil F, Calderon I, Fuentes JA, Rodas PI, Banawas S, Sarker MR, Paredes-Sabja D. 2016. Characterization of the adherence of *Clostridium difficile* spores: the integrity of the outermost layer affects adherence properties of spores of the epidemic strain R20291 to components of the intestinal mucosa. Front Cell Infect Microbiol 6:99. https://doi.org/10.3389/fcimb.2016.00099.
20. Castro-Córdova P, Mora-Uribe P, Reyes-Ramírez R, Cofré-Araneda G, Orozco-Aguilar J, Brito-Silva C, Mendoza-León MJ, Kuehne SA, Minton NP, Pizarro-Guajardo M, Paredes-Sabja D. 2021. Entry of spores into intestinal epithelial cells contributes to recurrence of *Clostridioides difficile* infection. Nat Commun 12:1140. https://doi.org/10.1038/s41467-021-21355-5.
21. Buckley A, Turner JR. 2018. Cell biology of tight junction barrier regulation and mucosal disease. Cold Spring Harb Perspect Biol 10:a029314. https://doi.org/10.1101/cshperspect.a029314.
22. Paradis T, Bègue H, Basmaciyan L, Dalle F, Bon F. 2021. Tight junctions as a key for pathogens invasion in intestinal epithelial cells. Int J Mol Sci 22:2506. https://doi.org/10.3390/ijms22052506.
23. Rubinstein MR, Wang X, Liu W, Hao Y, Cai G, Han YW. 2013. *Fusobacterium nucleatum* promotes colorectal carcinogenesis by modulating E-cadherin/β-catenin signaling via its FadA adhesin. Cell Host Microbe 14:195–206. https://doi.org/10.1016/j.chom.2013.07.012.
24. Anderton JM, Rajam G, Romero-Steiner S, Summer S, Kowalczyk AP, Carlone GM, Sampson JS, Ades EW. 2007. E-cadherin is a receptor for the common protein pneumococcal surface adhesin A (PsaA) of *Streptococcus pneumoniae*. Microb Pathog 42:225–236. https://doi.org/10.1016/j.micpath.2007.02.003.
25. Elmi A, Nasher F, Jagatia H, Gundogdu O, Bajaj-Elliott M, Wren B, Dorrell N. 2016. *Campylobacter jejuni* outer membrane vesicle-associated proteolytic activity promotes bacterial invasion by mediating cleavage of intestinal epithelial cell E-cadherin and occludin. Cell Microbiol 18:561–572. https://doi.org/10.1111/cmi.12534.
26. Mengaud J, Ohayon H, Gounon P, Mege R-M, Cossart P. 1996. E-cadherin is the receptor for internalin, a surface protein required for entry of *L. monocytogenes* into epithelial cells. Cell 84:923–932. https://doi.org/10.1016/s0092-8674(00)81070-3.
27. Ribet D, Cossart P. 2015. How bacterial pathogens colonize their hosts and invade deeper tissues. Microbes Infect 17:173–183. https://doi.org/10.1016/j.micinf.2015.01.004.
28. Calderon-Romero P, Castro-Cordova P, Reyes-Ramirez R, Milano-Cespedes M, Guerrero-Araya E, Pizarro-Guajardo M, Olguin-Araneda V, Gil F, Paredes-Sabja D. 2018. *Clostridium difficile* exosporium cysteine-rich proteins are essential for the morphogenesis of the exosporium layer, spore resistance, and affect *C. difficile* pathogenesis. PLoS Pathog 14:e1007199. https://doi.org/10.1371/journal.ppat.1007199.
29. Pizarro-Guajardo M, Diaz-Gonzalez F, Alvarez-Lobos M, Paredes-Sabja D. 2017. Characterization of chicken IgY specific to *Clostridium difficile* R20291 spores and the effect of oral administration in mouse models of initiation and recurrent disease. Front Cell Infect Microbiol 7:365. https://doi.org/10.3389/fcimb.2017.00365.
30. Schöttelndreier D, Langejürgen A, Lindner R, Genth H. 2020. Low density lipoprotein receptor-related protein-1 (LRP1) is involved in the uptake of *Clostridioides difficile* toxin A and serves as an internalizing receptor. Front Cell Infect Microbiol 10:565465. https://doi.org/10.3389/fcimb.2020.565465.
31. Tam J, Icho S, Utama E, Orrell KE, Gómez-Biagi RF, Theriot CM, Kroh HK, Rutherford SA, Lacy DB, Melnyk RA. 2020. Intestinal bile acids directly modulate the structure and function of *C. difficile* TcdB toxin. Proc Natl Acad Sci U S A 117:6792–6800. https://doi.org/10.1073/pnas.1916965117.
32. Landenberger M, Nieland J, Roeder M, Nørgaard K, Papatheodorou P, Ernst K, Barth H. 2021. The cytotoxic effect of *Clostridioides difficile* pore-forming toxin CDTb. Biochim Biophys Acta Biomembr 1863:183603. https://doi.org/10.1016/j.bbamem.2021.183603.
33. Aktories K, Schwan C, Jank T. 2017. *Clostridium difficile* toxin biology. Annu Rev Microbiol 71:281–307. https://doi.org/10.1146/annurev-micro-090816-093458.
34. Kroh HK, Chandrasekaran R, Zhang Z, Rosenthal K, Woods R, Jin X, Nyborg AC, Rainey GJ, Warrener P, Melnyk RA, Spiller BW, Lacy DB. 2018. A neutralizing antibody that blocks delivery of the enzymatic cargo of *Clostridium difficile* toxin TcdB into host cells. J Biol Chem 293:941–952. https://doi.org/10.1074/jbc.M117.813428.
35. Schwan C, Stecher B, Tzivelekidis T, van Ham M, Rohde M, Hardt WD, Wehland J, Aktories K. 2009. *Clostridium difficile* toxin CDT induces formation of microtubule-based protrusions and increases adherence of bacteria. PLoS Pathog 5:e1000626. https://doi.org/10.1371/journal.ppat.1000626.
36. Schwan C, Kruppke AS, Nolke T, Schumacher L, Koch-Nolte F, Kudryashev M, Stahlberg H, Aktories K. 2014. *Clostridium difficile* toxin CDT hijacks microtubule organization and reroutes vesicle traffic to increase pathogen adherence. Proc Natl Acad Sci U S A 111:2313–2318. https://doi.org/10.1073/pnas.1311589111.

37. Paredes-Sabja D, Cid-Rojas F, Pizarro-Guajardo M. 2022. Assembly of the exosporium layer in *Clostridioides difficile* spores. Curr Opin Microbiol 67:102137. https://doi.org/10.1016/j.mib.2022.01.008.
38. Pizarro-Guajardo M, Calderon-Romero P, Castro-Cordova P, Mora-Uribe P, Paredes-Sabja D. 2016. Ultrastructural variability of the exosporium layer of *Clostridium difficile* spores. Appl Environ Microbiol 82:2202–2209. https://doi.org/10.1128/AEM.03410-15.
39. Pizarro-Guajardo M, Calderon-Romero P, Paredes-Sabja D. 2016. Ultrastructure variability of the exosporium layer of *Clostridium difficile* spores from sporulating cultures and biofilms. Appl Environ Microbiol 82:5892–5898. https://doi.org/10.1128/AEM.01463-16.
40. Pizarro-Guajardo M, Calderón-Romero P, Romero-Rodríguez A, Paredes-Sabja D. 2020. Characterization of exosporium layer variability of *Clostridioides difficile* spores in the epidemically relevant strain R20291. Front Microbiol 11:1345. https://doi.org/10.3389/fmicb.2020.01345.
41. Pizarro-Guajardo M, Olguin-Araneda V, Barra-Carrasco J, Brito-Silva C, Sarker MR, Paredes-Sabja D. 2014. Characterization of the collagen-like exosporium protein, BclA1, of *Clostridium difficile* spores. Anaerobe 25:18–30. https://doi.org/10.1016/j.anaerobe.2013.11.003.
42. Phetcharaburanin J, Hong HA, Colenutt C, Bianconi I, Sempere L, Permpoonpattana P, Smith K, Dembek M, Tan S, Brisson MC, Brisson AR, Fairweather NF, Cutting SM. 2014. The spore-associated protein BclA1 affects the susceptibility of animals to colonization and infection by *Clostridium difficile*. Mol Microbiol 92:1025–1038. https://doi.org/10.1111/mmi.12611.
43. Lessa FC, Mu Y, Bamberg WM, Beldavs ZG, Dumyati GK, Dunn JR, Farley MM, Holzbauer SM, Meek JI, Phipps EC, Wilson LE, Winston LG, Cohen JA, Limbago BM, Fridkin SK, Gerding DN, McDonald LC. 2015. Burden of *Clostridium difficile* infection in the United States. N Engl J Med 372:825–834. https://doi.org/10.1056/NEJMoa1408913.
44. Kelly CP. 2012. Can we identify patients at high risk of recurrent *Clostridium difficile* infection? Clin Microbiol Infect 18:21–27. https://doi.org/10.1111/1469-0691.12046.
45. Zhang S, Palazuelos-Munoz S, Balsells EM, Nair H, Chit A, Kyaw MH. 2016. Cost of hospital management of Clostridium difficile infection in United States—a meta-analysis and modelling study. BMC Infect Dis 16:447. https://doi.org/10.1186/s12879-016-1786-6.
46. Nikitas G, Deschamps C, Disson O, Niault T, Cossart P, Lecuit M. 2011. Transcytosis of *Listeria monocytogenes* across the intestinal barrier upon specific targeting of goblet cell accessible E-cadherin. J Exp Med 208:2263–2277. https://doi.org/10.1084/jem.20110560.
47. Gessain G, Tsai YH, Travier L, Bonazzi M, Grayo S, Cossart P, Charlier C, Disson O, Lecuit M. 2015. PI3-kinase activation is critical for host barrier permissiveness to *Listeria monocytogenes*. J Exp Med 212:165–183. https://doi.org/10.1084/jem.20141406.
48. Pentecost M, Otto G, Theriot JA, Amieva MR. 2006. *Listeria monocytogenes* invades the epithelial junctions at sites of cell extrusion. PLoS Pathog 2:e3. https://doi.org/10.1371/journal.ppat.0020003.
49. Pentecost M, Kumaran J, Ghosh P, Amieva MR. 2010. *Listeria monocytogenes* internalin B activates junctional endocytosis to accelerate intestinal invasion. PLoS Pathog 6:e1000900. https://doi.org/10.1371/journal.ppat.1000900.
50. Singh B, Su YC, Riesbeck K. 2010. Vitronectin in bacterial pathogenesis: a host protein used in complement escape and cellular invasion. Mol Microbiol 78:545–560. https://doi.org/10.1111/j.1365-2958.2010.07373.x.
51. Henderson B, Nair S, Pallas J, Williams MA. 2011. Fibronectin: a multidomain host adhesin targeted by bacterial fibronectin-binding proteins. FEMS Microbiol Rev 35:147–200. https://doi.org/10.1111/j.1574-6976.2010.00243.x.
52. Hamzaoui N, Kernéis S, Caliot E, Pringault E. 2004. Expression and distribution of beta1 integrins in in vitro-induced M cells: implications for *Yersinia* adhesion to Peyer's patch epithelium. Cell Microbiol 6:817–828. https://doi.org/10.1111/j.1462-5822.2004.00391.x.
53. Clark MA, Hirst BH, Jepson MA. 1998. M-cell surface beta1 integrin expression and invasin-mediated targeting of *Yersinia pseudotuberculosis* to mouse Peyer's patch M cells. Infect Immun 66:1237–1243. https://doi.org/10.1128/IAI.66.3.1237-1243.1998.
54. Diaz-Gonzalez F, Milano M, Olguin-Araneda V, Pizarro-Cerda J, Castro-Cordova P, Tzeng SC, Maier CS, Sarker MR, Paredes-Sabja D. 2015. Protein composition of the outermost exosporium-like layer of *Clostridium difficile* 630 spores. J Proteomics 123:1–13. https://doi.org/10.1016/j.jprot.2015.03.035.
55. Kelly CP, Poxton IR, Shen J, Wilcox MH, Gerding DN, Zhao X, Laterza OF, Railkar R, Guris D, Dorr MB. 2020. Effect of endogenous *Clostridioides difficile* toxin antibodies on recurrence of *C. difficile* infection. Clin Infect Dis 71:81–86. https://doi.org/10.1093/cid/ciz809.
56. Ng YK, Ehsaan M, Philip S, Collery MM, Janoir C, Collignon A, Cartman ST, Minton NP. 2013. Expanding the repertoire of gene tools for precise manipulation of the *Clostridium difficile* genome: allelic exchange using *pyrE* alleles. PLoS One 8:e56051. https://doi.org/10.1371/journal.pone.0056051.
57. Wüst J, Sullivan NM, Hardegger U, Wilkins TD. 1982. Investigation of an outbreak of antibiotic-associated colitis by various typing methods. J Clin Microbiol 16:1096–1101. https://doi.org/10.1128/jcm.16.6.1096-1101.1982.
58. Chandrasekaran R, Kenworthy AK, Lacy DB. 2016. *Clostridium difficile* toxin A undergoes clathrin-independent, PACSIN2-dependent endocytosis. PLoS Pathog 12:e1006070. https://doi.org/10.1371/journal.ppat.1006070.